ANTICANCER RESEARCH *44*: 687-694 (2024)
doi:10.21873/anticanres.16859

Influence of Respiratory Motion on Dose Distribution in Gastric Mucosa-associated Lymphoid Tissue Lymphoma Radiotherapy

TADASHI MATSUMOTO[1], RYO TOYA[1,2], YOSHINOBU SHIMOHIGASHI[3], KOHSEI YAMAGUCHI[1], TAKAHIRO WATAKABE[1], TOMOHIKO MATSUYAMA[1], YOSHIYUKI FUKUGAWA[1], YUDAI KAI[3] and NATSUO OYA[1]

[1]*Department of Radiation Oncology, Faculty of Life Sciences, Kumamoto University, Kumamoto, Japan;*
[2]*Department of Radiological Sciences, Graduate School of Biomedical Sciences, Nagasaki University, Nagasaki, Japan;*
[3]*Department of Radiological Technology, Kumamoto University Hospital, Kumamoto, Japan*

Abstract. *Background/Aim: The present study investigated the effect of respiratory motion on planned radiotherapy (RT) dose for gastric mucosa-associated lymphoid tissue (MALT) lymphoma using four-dimensional dose (4D-dose) accumulation. Patients and Methods: 4D-computed tomography (4D-CT) images of 10 patients with gastric MALT lymphomas were divided into 10 respiratory phases. Further, the 3D-dose was calculated using 3D conformal RT (3D-CRT) and volumetric modulated arc therapy (VMAT) plans based on the average intensity projection (AIP) images. Then, both plans were recalculated according to each phase image. Moreover, the dose distributions in each phase were transferred to the AIP images using deformable image registration. The 4D-dose distribution was calculated by summing the doses of each phase, and it was compared with the dosimetric parameters of the 3D-dose distribution. Results: For 3D-CRT, the D_{95} and D_{99} of the 4D-dose in the planning target volume (PTV) were significantly lower than those of the 3D-dose, with mean differences of 0.2 (p=0.009) and 0.1 Gy (p=0.021), respectively. There were no significant differences in the other PTV and organ-at-risk dosimetric parameters of 3D-CRT or in any dosimetric parameters of VMAT between the 3D- and 4D-dose distributions. Conclusion: The effect of respiratory motion on the planned 3D-CRT and VMAT dose distributions for gastric MALT lymphoma is minimal and clinically negligible.*

Correspondence to: Ryo Toya, Department of Radiological Sciences, Graduate School of Biomedical Sciences, Nagasaki University, 1-7-1 Sakamoto, Nagasaki, 852-8501, Japan. Tel: +81 958197354, Fax: +81 958197357, e-mail: toya@nagasaki-u.ac.jp

Key Words: Gastric mucosa-associated lymphoid tissue lymphoma, radiotherapy, four-dimensional dose, volumetric modulated arc therapy, four-dimensional computed tomography, respiratory motion, deformable image registration.

Mucosa-associated lymphoid tissue (MALT) lymphoma can arise from any part of the human body, with the stomach being the most common site. Gastric MALT lymphomas are commonly found within the stomach, with stage IE accounting for 70%-80% of cases (1). Radiotherapy (RT) is the primary treatment option among *Helicobacter pylori* (HP)-positive patients who do not respond to eradication therapy, HP-positive patients with certain genetic mutations, and HP-negative patients (2). RT for gastric MALT lymphoma can achieve a local control rate of >90%, and a prescribed dose of 30 Gy in 20 fractions is recommended. Gastric MALT lymphoma patients can have a good prognosis after RT (3). Therefore, the organ-at-risk (OAR) doses should be maintained at the lowest possible value.

The stomach is a large organ surrounded by various radiosensitive organs, including the kidneys, liver, spinal cord, small bowel, and duodenum. RT for gastric MALT lymphoma is challenging because it requires a huge target volume to be irradiated while avoiding these radiosensitive organs. Traditionally, three-dimensional conformal RT (3D-CRT) is widely used for the treatment (4). In the last decade, volumetric modulated arc therapy (VMAT) has been increasingly used for abdominal tumors (5, 6). VMAT can deliver beams while modifying the dose rate, field shape, and gantry rotation speed (7). A previous study on gastric MALT lymphoma showed that the VMAT plan is superior to the 3D-CRT plan in terms of homogeneity and conformity of the planning target volume (PTV) while reducing the OAR doses (8). Meanwhile, the abdominal organs change position with respiration (9), possibly affecting the planned dose distribution of the target volumes and OARs (10, 11). Thus, the remaining concern is the influence of respiratory motion on the dose distribution of treatment plans for gastric MALT lymphoma.

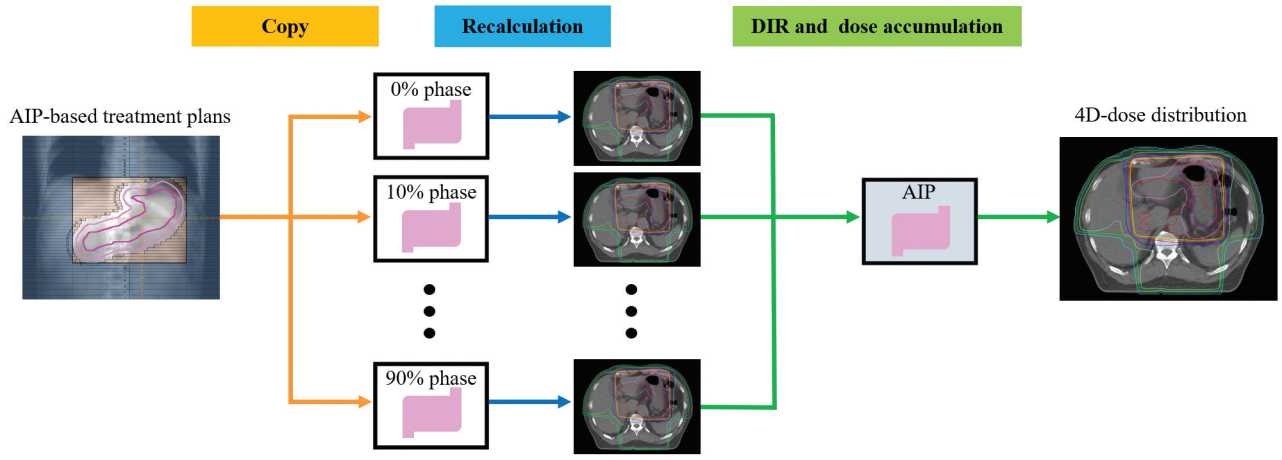

Figure 1. *Flow chart of the 4D-dose accumulation. PTV (pink) and CTV-4D (purple) are displayed on the beam's eye view of the average intensity projection (AIP)-based treatment plans. DIR: Deformable image registration.*

Four-dimensional computed tomography (4D-CT) imaging, which provides morphologic information about the structures in each respiratory phase, is a useful technique for assessing the respiratory changes of the target volume and OARs (12). Additionally, deformable image registration (DIR) techniques, which yield tissue deformation by resolving the voxel-to-voxel changes between two images, have recently improved (13). These technical advancements facilitate the use of four-dimensional dose (4D-dose) accumulation, which involves the integration of the 3D-dose distribution per respiratory phase produced by 4D-CT imaging onto the target image using DIR. Currently, 4D-dose accumulation is the standard method used for assessing the effect of respiratory changes on the treatment plan's dose distribution (14). However, studies examining the effect of respiratory changes on dose distribution in RT planning for gastric MALT lymphoma using 4D-dose accumulation are lacking. Thus, the current study aimed to investigate the effect of respiratory motion on the planned RT dose for gastric MALT lymphomas using 4D-dose accumulation.

Patients and Methods

Patients. The 4D-CT images of 10 consecutive patients with stage IE gastric MALT lymphoma [7 men and 3 women with a median age of 63 (range=52-72) years] who received RT at our hospital between February 2019 and October 2021 were used in the present study.

CT simulation. The detailed information on CT simulation has been described previously (8). In our study, the patients fasted for at least 8 h before the CT simulation. 4D-CT imaging was performed for RT planning, and the images were divided into 10 respiratory phases. The average intensity projection (AIP) of the CT images was created based on all respiratory phase projection data. All CT images were exported to the treatment planning system (RayStation Clinical version 10A SP1, RaySearch Laboratories, Stockholm, Sweden) and registered by the hardware arrangement.

Definition of contours. To define the target volumes and OARs, the Radiation Therapy Oncology Group contouring atlases were used (15). Contouring was performed *via* a consensus decision between two radiation oncologists with 6 and 18 years of experience. According to the endoscopic examination results, we determined the gross tumor volume. The clinical target volume (CTV) was defined as the volume of the whole stomach (stomach CTV), from the gastro–esophageal junction to the duodenal bulb. The CTV was delineated on the AIP and 10 respiratory phase CT images. The CTV-4D, defined as the volume covering the stomach's 10 respiratory phases, was delineated on the AIP CT image data sets using fused 4D-CT images (9). Based on the guideline recommendation, the PTV was generated by adding a 10-mm margin for CTV-4D, which included intra- and inter-fractional changes in stomach volume, respiratory movement, and set-up errors (16). The OARs, including the kidneys, liver, spinal cord, small bowel, and duodenum, were delineated on the AIP and each respiratory phase CT image.

Treatment planning. The 3D-CRT and VMAT plans were based on the AIP CT images. For irradiation in both plans, a linear accelerator (TrueBeam Edge; Varian Medical Systems, Palo Alto, CA, USA) was used. The dose of 30 Gy in 20 fractions was prescribed. The 3D-CRT plan comprised a four-box field with a 10-MV X-ray (8). The multileaf collimator was adjusted with a 5-mm leaf margin in all directions from the PTV. The VMAT plan comprised a single full arc with a 6-MV X-ray (8). The goals of each VMAT plan were as follows: minimum coverage dose for 95% of the PTV (D_{95}) should be >95% of the prescribed dose; mean dose (Dmean) in the liver, <12.5 Gy; D_{mean} of each kidney, <10 Gy; maximum dose (D_{max}) of the spinal cord, <30 Gy; and D_{max} of the small bowel and duodenum, <31.5 Gy (17). The collapsed cone convolution algorithm with a 2.0-mm grid size was used for dose calculation.

4D-dose accumulation. The 4D-dose accumulation workflow is shown in Figure 1. The AIP-based treatment plans were copied onto the 4D-CT images of each phase without changing the planning parameters. The dose was then recalculated based on each 4D-CT phase image. Subsequently, DIR was performed to produce a 4D-dose distribution. In the present study, an anatomically constrained

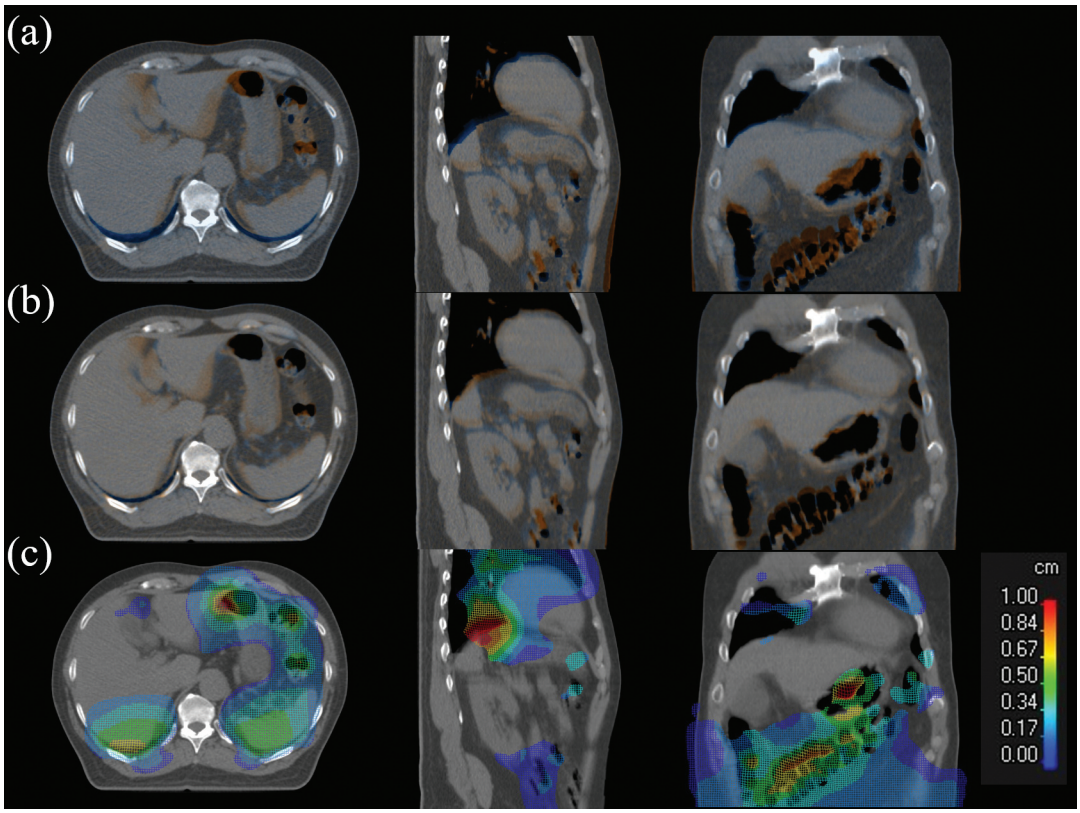

Figure 2. *The fusion views and deformable vector fields from the 0% phase to the average intensity projection (AIP) images. (A) Before deformable image registration (DIR). (B) After DIR. The blue and orange colors represent the AIP and 0% phase images, respectively. (C) Displacement field color table. The blue and red meshes indicate the lower and higher magnitudes, respectively.*

deformation algorithm was used for DIR (13). Using the AIP as a reference image, each phase image was deformed to produce a deformation map (Figure 2). To confirm whether the target volumes and OARs were deformed appropriately, a visual inspection was performed (18). Each dose distribution was accumulated with equal weighting equivalent to 1/10th of the prescribed dose on a reference image using the corresponding deformation map. Moreover, the dose difference percentage was estimated by subtracting the 3D-dose distribution from the 4D-dose distribution.

Dosimetric parameters for plan evaluation. Plan evaluation was performed using a dose–volume histogram. D_{95} was used to evaluate the PTV coverage. The homogeneity index (HI) and conformity index (CI) of the PTV were calculated using equations [1] and [2], which are as follows (8):

$$HI = \frac{D_1 - D_{99}}{D_p} \quad [1],$$

$$CI = \frac{BV_{95}}{PTV} \quad [2],$$

where D_1 and D_{99} are the minimum doses covering 1% and 99% of the PTV, respectively, and D_p is the prescription dose. D_1 and D_{99} were used to evaluate the maximum and minimum doses of the PTV, respectively. BV95 is the body volume receiving 95% of the prescribed dose.

The D_{mean} and D_{max} were used for evaluating the parallel organs (kidneys and liver) and serial organs (spinal cord, small bowel, and duodenum), respectively.

Stomach CTV center of mass displacement. The coordinates of the center of mass (COM) of the stomach CTV in the 0% phase image were set as zero. In each patient, the displacement from the 0% phase images to the other respiratory phase images for the anterior–posterior (AP), left–right (LR), and superior–inferior (SI) directions was calculated.

Statistical analysis. To compare the 3D- and 4D-dose distributions, we performed the Wilcoxon signed-rank test. The Statistical Package for the Social Sciences (version 26.0; IBM, Armonk, NY, USA) was used for the statistical analyses. A p-value of <0.05 was considered statistically significant.

Ethics approval and consent to participate. The present study was approved by Institutional Ethical Review Board (Kumamoto University Hospital Review Board No. 1878). All patients were enrolled with prior written informed consent for this study and consent regarding the use of image data. All research procedures were performed in accordance with the Declaration of Helsinki, related guidelines, and regulations.

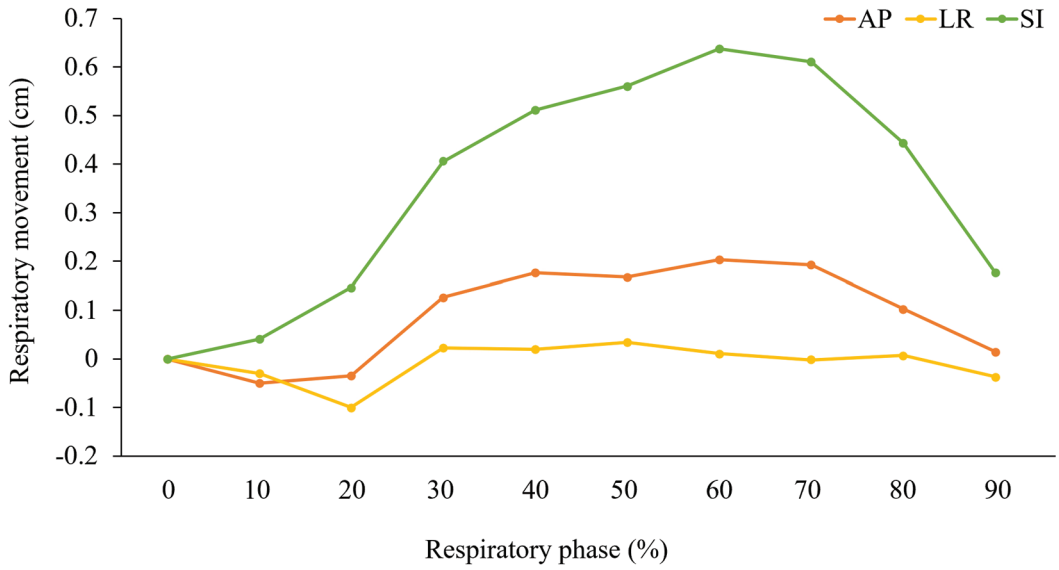

Figure 3. *Respiratory displacement in each respiratory phase for the center of mass of the clinical target volume.*

Table I. *Respiratory displacement of the center of mass of the clinical target volume in 10 patients.*

	Patient no.										Average (cm)	Range (cm)	SD (cm)
Direction	1	2	3	4	5	6	7	8	9	10			
AP	0.30	0.40	0.42	0.38	0.53	0.60	0.32	0.32	0.47	0.35	0.41	0.30-0.60	0.10
LR	0.85	0.31	0.29	0.19	0.34	0.32	0.34	0.38	0.32	0.17	0.35	0.17-0.85	0.19
SI	0.42	0.73	0.45	0.63	0.70	0.72	0.73	0.97	0.80	0.55	0.67	0.42-0.97	0.16

AP: Anterior–posterior; LR: left–right; SI: superior–inferior; SD: standard deviation; 4D-CT: four-dimensional computed tomography.

Results

Stomach displacements. Figure 3 and Table I show the stomach CTV COM respiratory displacement. The average (±standard deviation) respiratory displacement in 10 patients in the AP, LR, and SI directions were 0.41 (±0.10), 0.35 (±0.19), and 0.67 (±0.16) cm, respectively.

Dosimetric parameters. Table II shows the dosimetric parameters of the 3D- and 4-D doses. Figure 4 depicts an example of the dose distribution in the 3D-CRT and VMAT plans. For the 3D-CRT plan, the D_{95} and D_{99} of the 4D-dose in PTV were significantly lower than those of the 3D-dose, with mean difference of 0.2 (p=0.009) and 0.1 Gy (p=0.021), respectively. There were no significant differences in the other PTV and OAR dosimetric parameters of the 3D-CRT plan or any dosimetric parameters of the VMAT plan between the 3D- and 4D-dose distributions.

Discussion

We evaluated the 4D-dose distribution of 3D-CRT and VMAT plans delivered to patients with gastric MALT lymphoma using 4D-dose accumulation with 4D-CT and DIR. The results revealed that the effect of respiratory motion on the planned dose distributions for gastric MALT lymphoma is minimal and clinically negligible in both plans.

In the current study, 4D-dose accumulation was used for evaluating the 4D-dose distribution of OARs and PTV (19). Uchinami *et al*. have assessed stomach motion based on the dosimetric parameters in 10 gastric lymphoma patients receiving intensity-modulated RT. The isocenter shift method was used, wherein the isocenter and beams were shifted three-dimensionally in the opposite direction of the actual organ motion to reproduce the stomach motion in the treatment planning system (20). They reported that the dose reduction in CTV is clinically low with <1% of the planned

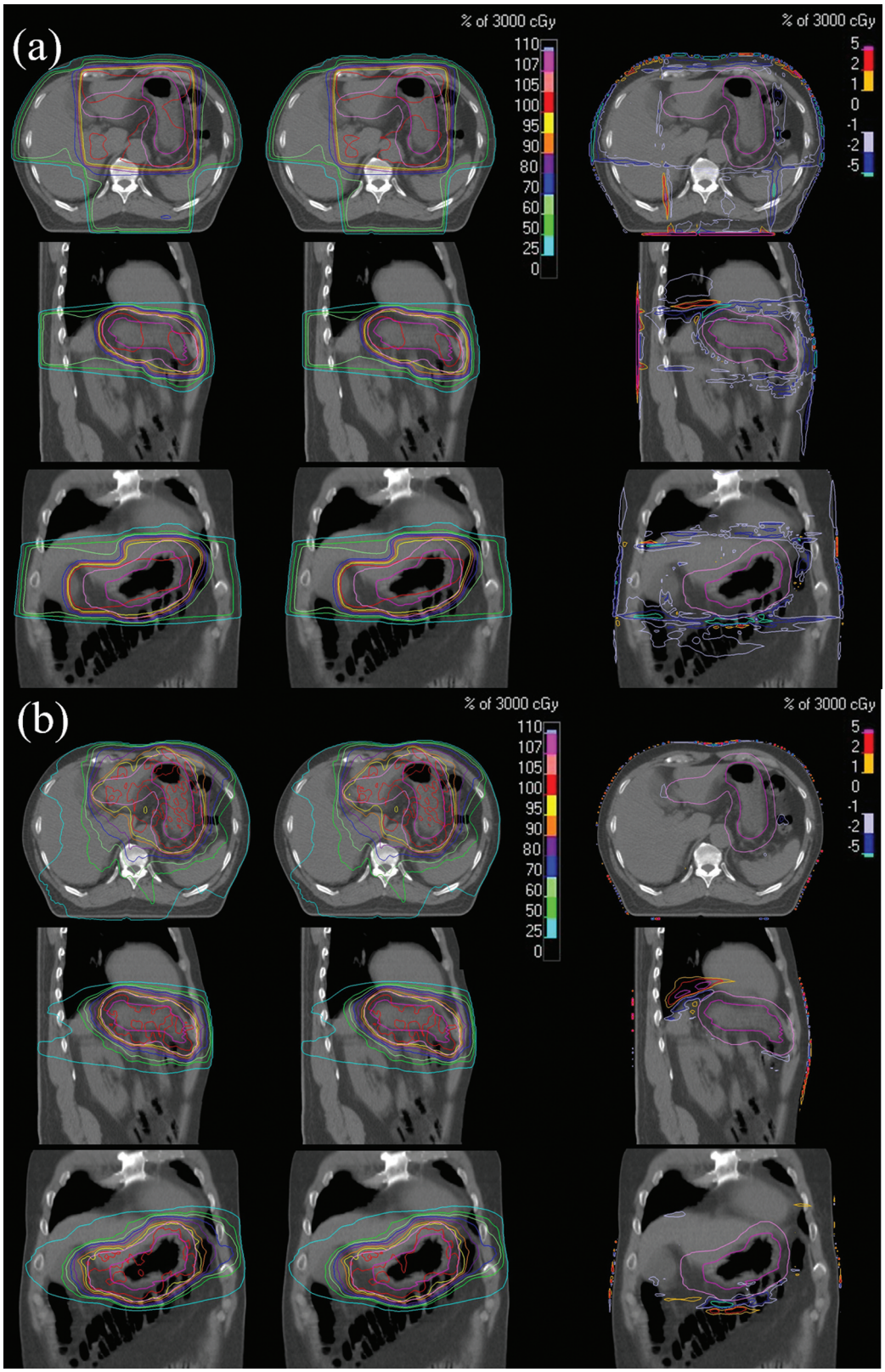

Figure 4. *Examples of the dose distributions for (A) three-dimensional (3D) conformal radiotherapy and (B) volumetric modulated arc therapy plans. Left: 3D-dose; center: 4D-dose; right: dose difference (%) between the 3D- and 4D-dose distributions (4D-dose minus 3D-dose).*

Table II. *Dosimetric parameters of the 3D- and 4D-dose distributions.*

		3D-CRT			VMAT		
		3D-dose	4D-dose	*p*-Value*	3D-dose	4D-dose	*p*-Value*
PTV	D_{95} (Gy)	28.7±0.5	28.6±0.5	0.021	28.7±0.2	28.7±0.2	>0.999
	D_{99} (Gy)	27.5±0.9	27.3±0.8	0.009	27.8±0.4	27.7±0.4	0.621
	D_1 (Gy)	31.6±0.5	31.6±0.4	>0.999	31.1±0.3	31.2±0.2	>0.999
	HI	0.14±0.04	0.14±0.04	0.100	0.11±0.02	0.11±0.02	>0.999
	CI	1.5±0.2	1.5±0.2	0.095	1.1±0.1	1.1±0.1	>0.999
Liver	D_{mean} (Gy)	15.7±2.0	15.7±2.0	0.586	11.1±0.7	11.1±0.6	0.174
Right kidney	D_{mean} (Gy)	3.9±2.0	3.9±2.0	0.149	5.3±2.8	5.3±2.8	>0.999
Left kidney	D_{mean} (Gy)	6.8±6.0	6.8±6.0	0.098	6.2±2.8	6.2±2.8	>0.999
Spinal cord	D_{max} (Gy)	23.7±4.9	23.6±4.9	0.269	20.9±1.4	21.0±1.5	0.371
Small bowel	D_{max} (Gy)	30.3±0.8	30.3±0.8	>0.999	30.5±1.2	30.4±1.1	0.233
Duodenum	D_{max} (Gy)	30.1±1.0	30.1±1.0	0.854	31.0±0.3	31.1±0.4	>0.999

3D-CRT: Three-dimensional conformal radiotherapy; VMAT: volumetric modulated arc therapy; 3D-dose: three-dimensional dose; 4D-dose: four-dimensional dose; PTV: planning target volume; D_x: minimum coverage dose of x% of the PTV; HI: homogeneity index; CI: conformity index; D_{mean}: mean dose; D_{max}: maximum dose. *Wilcoxon signed-rank test.

dose. However, the OAR doses were not evaluated because the OAR's 4D-dose could not be calculated using the isocenter shift method. We were able to assess the 4D-dose distribution of PTV and OARs using DIR.

In the 3D-CRT plan, our results showed that the dose coverage of PTV and the minimum dose to PTV in the 4D-dose distribution were slightly lower than those in the 3D-dose distribution, which may be due to the dose gradient at the PTV's peripheral part. Mankinen *et al*. compared the planned dose between VMAT and 3D-CRT for 10 whole-breast irradiation plans at free-breathing (21). Using 4D-dose accumulation, they found that the PTV coverage mainly decreased in areas with steep dose fall-off gradients. The 3D-CRT plan had a steeper dose gradient than the VMAT plan in the area corresponding to the edge of the field around the PTV, which might lead to a significant dose reduction caused by respiratory motions in the 4D-dose distribution of the 3D-CRT plan. However, the difference was ≤0.2 Gy with <1% of the prescribed dose, and the other dosimetric parameters of 3D-CRT were not significantly different between the 3D- and 4D-doses. We confirmed that, in the 3D-CRT plan, the clinical impact of the differences in dose distribution caused by the respiratory changes is clinically negligible. Furthermore, for the VMAT plan, we confirmed that the dosimetric changes in PTV and OARs caused by the respiratory motion are totally negligible. Considering that the dose distribution of VMAT is significantly better than that of 3D-CRT, VMAT should be aggressively introduced into RT for gastric MALT lymphoma (8).

Only a few studies have quantified the gastric respiratory motion of COM. Uchinami *et al*. assessed the intrafraction gastric motion of COM in 10 patients with stomach lymphomas *via* 4D-CT imaging at free-breathing (18). Their results showed that the average respiratory motions of the stomach COM in the AP, LR, and SI directions were 0.41 (±0.14), 0.29 (±0.13), and 1.01 (±0.45) cm, respectively. Similar to Uchinami *et al*.'s results, our findings showed that the stomach CTV COM showed the largest displacement in the SI direction (20).

The current study has some limitations. First, although the expiration phase is practically longer than the inspiration phase, we calculated the 4D-dose distribution *via* equal weighting for each respiratory phase (22). Second, as we performed planning based on the single 4D-CT imaging, the effects of inter- and intrafractional changes of the structures on dose distribution were not considered. Third, although we evaluated the stomach CTV COM respiratory displacement, we were unable to evaluate the shift position of the CTV contours. Fourth, the interplay effects of VMAT were not considered. However, a previous study has suggested the minimal impact of interplay effect in cases with large irradiated fields or a large number of irradiations, such as gastric MALT lymphoma (23).

Conclusion

In both 3D-CRT and VMAT plans, the difference in the dose distributions produced by the respiratory motion is clinically negligible. Considering that VMAT's dose distribution is significantly better than that of 3D-CRT, VMAT should be aggressively introduced into RT for patients with gastric MALT lymphoma.

Conflicts of Interest

The Authors declare that they have no competing interests in relation to this study.

Authors' Contributions

TM developed the study design; collected, analyzed, and interpreted the data; performed the statistical analysis; and drafted the manuscript. RT developed the study design; collected, analyzed, and interpreted the data; and revised the manuscript. YS developed the study design; performed radiotherapy planning; and collected, analyzed, and interpreted the data. KY, TW, and YK developed the study design and collected and interpreted the data. TM, YF, and NO developed the study design and interpreted the data. All Authors have read and approved the final manuscript.

Funding

No funds, grants, or other support was received.

References

1 Raderer M, Kiesewetter B, Ferreri AJM: Clinicopathologic characteristics and treatment of marginal zone lymphoma of mucosa-associated lymphoid tissue (MALT lymphoma). CA Cancer J Clin 66(2): 152-171, 2016. DOI: 10.3322/caac.21330

2 National Comprehensive Cancer Network. NCCN clinical practice guidelines in oncology, b-cell lymphomas (version 6). 2023. Available at: https://www.nccn.org/guidelines/guidelines detail?category=1&id=1480 [Last accessed on November 30, 2023]

3 Ohkubo Y, Saito Y, Ushijima H, Onishi M, Kazumoto T, Saitoh JI, Kubota N, Kobayashi H, Maseki N, Nishimura Y, Kurosumi M: Radiotherapy for localized gastric mucosa-associated lymphoid tissue lymphoma: long-term outcomes over 10 years. J Radiat Res 58(4): 537-542, 2017. DOI: 10.1093/jrr/rrw044

4 Della Biancia C, Hunt M, Furhang E, Wu E, Yahalom J: Radiation treatment planning techniques for lymphoma of the stomach. Int J Radiat Oncol Biol Phys 62(3): 745-751, 2005. DOI: 10.1016/j.ijrobp.2004.10.025

5 Toya R, Saito T, Kai Y, Shiraishi S, Matsuyama T, Watakabe T, Sakamoto F, Tsuda N, Shimohigashi Y, Yamashita Y, Oya N: Impact of (99m)Tc-GSA SPECT image-guided inverse planning on dose-function histogram parameters for stereotactic body radiation therapy planning for patients with hepatocellular carcinoma: a dosimetric comparison study. Dose Response 17(1): 1559325819832149, 2019. DOI: 10.1177/1559325819832149

6 Toya R, Watakabe T, Kai Y, Matsuyama T, Fukugawa Y, Matsumoto T, Shiraishi S, Shimohigashi Y, Saeki S, Sakagami T, Hirai T, Oya N: Implementation of (99m)Tc-GSA SPECT image-guided inverse planning into palliative radiotherapy for diffuse liver metastases: a novel approach. In Vivo 36(3): 1523-1526, 2022. DOI: 10.21873/invivo.12862

7 Kai Y, Toya R, Saito T, Kuraoka A, Shimohigashi Y, Nakaguchi Y, Maruyama M, Murakami R, Yamashita Y, Oya N: Plan quality and delivery time comparisons between volumetric modulated arc therapy and intensity modulated radiation therapy for scalp angiosarcoma: A planning study. J Med Radiat Sci 65(1): 39-47, 2018. DOI: 10.1002/jmrs.239

8 Matsumoto T, Toya R, Shimohigashi Y, Watakabe T, Matsuyama T, Saito T, Fukugawa Y, Kai Y, Oya N: Plan quality comparisons between 3D-CRT, IMRT, and VMAT based on 4D-CT for gastric MALT lymphoma. Anticancer Res 41(8): 3941-3947, 2021. DOI: 10.21873/anticanres.15190

9 Shimohigashi Y, Toya R, Saito T, Kono Y, Doi Y, Fukugawa Y, Watakabe T, Matsumoto T, Kai Y, Maruyama M, Oya N: Impact of four-dimensional cone-beam computed tomography on target localization for gastric mucosa-associated lymphoid tissue lymphoma radiotherapy: reducing planning target volume. Radiat Oncol 16(1): 14, 2021. DOI: 10.1186/s13014-020-01734-w

10 Velec M, Moseley JL, Eccles CL, Craig T, Sharpe MB, Dawson LA, Brock KK: Effect of breathing motion on radiotherapy dose accumulation in the abdomen using deformable registration. Int J Radiat Oncol Biol Phys 80(1): 265-272, 2011. DOI: 10.1016/j.ijrobp.2010.05.023

11 Sasaki M, Nakamura M, Mukumoto N, Goto Y, Ishihara Y, Nakata M, Sugimoto N, Mizowaki T: Variation in accumulated dose of volumetric-modulated arc therapy for pancreatic cancer due to different beam starting phases. J Appl Clin Med Phys 20(10): 118-126, 2019. DOI: 10.1002/acm2.12720

12 Jang JW, Brown JG, Mauch PM, Ng AK: Four-dimensional *versus* 3-dimensional computed tomographic planning for gastric mucosa associated lymphoid tissue lymphoma. Pract Radiat Oncol 3(2): 124-129, 2013. DOI: 10.1016/j.prro.2012.05.004

13 Weistrand O, Svensson S: The ANACONDA algorithm for deformable image registration in radiotherapy. Med Phys 42(1): 40-53, 2015. DOI: 10.1118/1.4894702

14 Ahanj M, Bissonnette JP, Heath E, McCann C: Robustness assessment of a novel IMRT planning method for lung radiotherapy. Phys Med 32(6): 749-757, 2016. DOI: 10.1016/j.ejmp.2016.03.013

15 Jabbour SK, Hashem SA, Bosch W, Kim TK, Finkelstein SE, Anderson BM, Ben-Josef E, Crane CH, Goodman KA, Haddock MG, Herman JM, Hong TS, Kachnic LA, Mamon HJ, Pantarotto JR, Dawson LA: Upper abdominal normal organ contouring guidelines and atlas: a Radiation Therapy Oncology Group consensus. Pract Radiat Oncol 4(2): 82-89, 2014. DOI: 10.1016/j.prro.2013.06.004

16 Yahalom J, Illidge T, Specht L, Hoppe RT, Li YX, Tsang R, Wirth A, International Lymphoma Radiation Oncology Group: Modern radiation therapy for extranodal lymphomas: Field and dose guidelines from the International Lymphoma Radiation Oncology group. Int J Radiat Oncol Biol Phys 92(1): 11-31, 2015. DOI: 10.1016/j.ijrobp.2015.01.009

17 Choi SH, Park SH, Lee JJB, Baek JG, Kim JS, Yoon HI: Combining deep-inspiration breath hold and intensity-modulated radiotherapy for gastric mucosa-associated lymphoid tissue lymphoma: Dosimetric evaluation using comprehensive plan quality indices. Radiat Oncol 14(1): 59, 2019. DOI: 10.1186/s13014-019-1263-7

18 Xu H, Gong G, Yin Y, Liu T: A preliminary investigation of re-evaluating the irradiation dose in hepatocellular carcinoma radiotherapy applying 4D CT and deformable registration. J Appl Clin Med Phys 22(2): 13-20, 2021. DOI: 10.1002/acm2.13111

19 Ohira S, Ueda Y, Hashimoto M, Miyazaki M, Isono M, Kamikaseda H, Masaoka A, Takashina M, Koizumi M, Teshima T: VMAT-SBRT planning based on an average intensity projection for lung tumors located in close proximity to the diaphragm: a phantom and clinical validity study. J Radiat Res 57(1): 91-97, 2016. DOI: 10.1093/jrr/rrv058

20 Uchinami Y, Suzuki R, Katoh N, Taguchi H, Yasuda K, Miyamoto N, Ito YM, Shimizu S, Shirato H: Impact of organ

motion on volumetric and dosimetric parameters in stomach lymphomas treated with intensity-modulated radiotherapy. J Appl Clin Med Phys 20(8): 78-86, 2019. DOI: 10.1002/acm2.12681

21 Mankinen M, Virén T, Seppälä J, Hakkarainen H, Koivumäki T: Dosimetric effect of respiratory motion on planned dose in whole-breast volumetric modulated arc therapy using moderate and ultra-hypofractionation. Radiat Oncol 17(1): 46, 2022. DOI: 10.1186/s13014-022-02014-5

22 Lujan AE, Larsen EW, Balter JM, Ten Haken RK: A method for incorporating organ motion due to breathing into 3D dose calculations. Med Phys 26(5): 715-720, 1999. DOI: 10.1118/1.598577

23 Edvardsson A, Nordström F, Ceberg C, Ceberg S: Motion induced interplay effects for VMAT radiotherapy. Phys Med Biol 63(8): 085012, 2018. DOI: 10.1088/1361-6560/aab957

Received December 12, 2023
Revised December 29, 2023
Accepted January 2, 2024